Pergamon

Geochimica et Cosmochimica Acta, Vol. 68, No. 21, pp. 4347–4361, 2004

0016-7037/04 $30.00 + .00

doi:10.1016/j.gca.2004.03.013

Effects of seawater carbonate ion concentration and temperature on shell U, Mg, and Sr in cultured planktonic foraminifera

ANN D. RUSSELL,[1,]* BÄRBEL HÖNISCH,[2,†] HOWARD J. SPERO,[1] and DAVID W. LEA[3]

[1]Department of Geology, University of California, Davis, CA 95616, USA
[2]Alfred Wegener Institute for Polar and Marine Research, Bremerhaven, Germany
[3]Department of Geological Sciences and the Marine Science Institute, University of California, Santa Barbara, CA 93106-9630, USA

(*Received July* 30, 2003; *accepted in revised form March* 10, 2004)

Abstract—We investigate the sensitivity of U/Ca, Mg/Ca, and Sr/Ca to changes in seawater $[CO_3^{2-}]$ and temperature in calcite produced by the two planktonic foraminifera species, *Orbulina universa* and *Globigerina bulloides,* in laboratory culture experiments. Our results demonstrate that at constant temperature, U/Ca in *O. universa* decreases by 25 ± 7% per 100 μmol $[CO_3^{2-}]$ kg^{-1}, as seawater $[CO_3^{2-}]$ increases from 110 to 470 μmol kg^{-1}. Results from *G. bulloides* suggest a similar relationship, but U/Ca is consistently offset by ~+40% at the same environmental $[CO_3^{2-}]$. In *O. universa,* U/Ca is insensitive to temperature between 15°C and 25°C. Applying the *O. universa* relationship to three U/Ca records from a related species, *Globigerinoides sacculifer,* we estimate that Caribbean and tropical Atlantic $[CO_3^{2-}]$ was 110 ± 70 μmol kg^{-1} and 80 ± 40 μmol kg^{-1} higher, respectively, during the last glacial period relative to the Holocene. This result is consistent with estimates of the glacial–interglacial change in surface water $[CO_3^{2-}]$ based on both modeling and on boron isotope pH estimates. In settings where the addition of U by diagenetic processes is not a factor, down-core records of foraminiferal U/Ca have potential to provide information about changes in the ocean's carbonate concentration.

Below ambient pH (pH < 8.2), Mg/Ca decreased by 7 ± 5% (*O. universa*) to 16 ± 6% (*G. bulloides*) per 0.1 unit increase in pH. Above ambient pH, the change in Mg/Ca was not significant for either species. This result suggests that Mg/Ca-based paleotemperature estimates for the Quaternary, during which surface-ocean pH has been at or above modern levels, have not been biased by variations in surface-water pH. Sr/Ca increased linearly by 1.6 ± 0.4% per 0.1 unit increase in pH. Shell Mg/Ca increased exponentially with temperature in *O. universa,* where Mg/Ca = 0.85 exp (0.096*T), whereas the change in Sr/Ca with temperature was within the reproducibility of replicate measurements. *Copyright © 2004 Elsevier Ltd*

1. INTRODUCTION

Over two decades ago, atmospheric pCO_2 records from ice cores from Greenland and Antarctica showed that glacial pCO_2 levels were approximately 30% lower than interglacial levels (Berner et al., 1979; Neftel et al., 1982; Barnola et al., 1987; Petit, 1999). Marine processes that alter the inventory or the distribution of total dissolved inorganic carbon (DIC = $[CO_2]$ + $[HCO_3]$ + $[CO_3^{2-}]$) and alkalinity in the ocean are considered the primary potential drivers of atmospheric pCO_2 change. Candidates to explain the observed atmospheric pCO_2 cycles generally include 1) processes that change the rates of $CaCO_3$ input and output to the ocean, and 2) processes that change the rates of organic carbon export by phytoplankton productivity or alternatively, the relative rain rates of organic carbon and $CaCO_3$ from the surface to the deep ocean (Broecker and Peng, 1982; Archer et al., 2000; Sigman and Boyle, 2000).

Proxies of carbonate system parameters would allow us to reconstruct changes in the distribution of carbon species in the surface and deep ocean, providing constraints necessary to evaluate the different mechanisms proposed to account for atmospheric CO_2 fluctuations. In regions of upwelling or high productivity, knowledge of both CO_{2aq} in the surface ocean and atmospheric pCO_2 from ice cores would allow us to calculate regional and temporal changes in the CO_2 flux between the atmosphere and the surface ocean. In the deep ocean, the ability to reconstruct vertical $[CO_3^{2-}]$ profiles would identify the relative positions of the carbonate saturation horizon and the calcite lysocline. This would provide an important constraint for evaluating the role of changes in the ratio of organic carbon to $CaCO_3$ in particulate matter exported to the deep sea (Archer and Maier-Reimer, 1994; Sigman et al., 1998).

A growing number of studies demonstrate relationships between various geochemical parameters recorded in calcium carbonate and changes in seawater $[CO_3^{2-}]$ or pH. For example, laboratory culture experiments at constant temperature showed that the shell $\delta^{18}O$ and $\delta^{13}C$ of four planktonic foraminiferal species (*G. bulloides, O. universa, G. sacculifer,* and *Globigerinoides ruber*) decrease with increasing $[CO_3^{2-}]$ (Spero et al., 1997; Bijma et al., 1998), with potentially important consequences for the interpretation of isotope records from deep-sea cores (Lea et al., 1999a; Spero et al., 1999). Similar experiments with *G. bulloides* and *O. universa* showed that shell Mg/Ca and Sr/Ca ratios also vary with pH. These changes were attributed to kinetic effects related to calcification rate (Lea et al., 1999b). The Zn/Ca and Cd/Ca ratios of benthic foraminifera are correlated with $\Delta[CO_3^{2-}]$, where $\Delta[CO_3^{2-}]$ is the offset between in situ $[CO_3^{2-}]$ and $[CO_3^{2-}]$ at saturation with calcite (Marchitto et al., 2000). Because the concentrations of Zn and Cd in seawater may be assumed constant over time,

---

* Author to whom correspondence should be addressed (russell@geology.ucdavis.edu).

† *Present address:* Lamont Doherty Earth Observatory, Palisades, NY 10964-1000, USA.

these ratios in benthic foraminifera may permit reconstruction of bottom-water [CO_3^{2-}] (Marchitto et al., 2001).

Recently, variations in shell weight of planktonic foraminifera (for a restricted size range) have been used to reconstruct changes in surface water [CO_3^{2-}] (Barker and Elderfield, 2002). Previous workers used variations in shell weight of planktonic foraminifera to reconstruct bottom-water [CO_3^{2-}], based on the observation that shell weights decrease as a result of postdepositional dissolution (Lohmann, 1995). This approach assumes that no variation in the initial shell weight occurs as a result of differences in environmental conditions of shell growth. However, it is now recognized that initial shell weights do vary as a result of different ambient conditions, including [CO_3^{2-}], light intensity, and temperature, thereby complicating the use of this relationship as either a proxy for bottom-water [CO_3^{2-}] (dissolution) or for surface water [CO_3^{2-}] (Bijma et al., 2002; Broecker and Clark, 2001, 2002, 2003).

The influence of [CO_3^{2-}] over the aqueous geochemistry of uranium, largely as a result of the formation of highly stable complexes between uranyl ion (UO_2^{2+}) and [CO_3^{2-}], is well known. Formation of carbonate complexes increases the solubility of uranium-containing minerals and decreases the extent of adsorption onto surfaces, thereby increasing the mobility of U in the aqueous environment (Langmuir, 1978). A number of researchers have speculated on the relationship between U in calcium carbonate and the inorganic carbon content of the solution from which it precipitated. The correlation between U and total carbon concentrations in saline lakes of California and Nevada led to the suggestion that U in corals might serve as a tracer of changes in the total carbon content of seawater (Broecker and Peng, 1982). Variations in the U/Ca of reef-building corals are consistent with estimated changes in seawater [CO_3^{2-}], although these variations are also consistent with a temperature control (Min et al., 1995; Shen and Dunbar, 1995). In a study of U in inorganic calcite cements from a Bahamian island ooid formation, the U content of cements in the vadose zone was much lower than that in the saturated aquifer. One explanation for this difference proposed by the authors was a higher pCO_2 within the saturated aquifer, lowering [CO_3^{2-}] and thus raising the U content of calcite cements (Chung and Swart, 1990). Experimental evidence also exists for a pH control on the incorporation of U into inorganic aragonite (Kitano and Oomori, 1971; Meece and Benninger, 1993) and calcite (Kitano and Oomori, 1971).

Previous work showed that the U/Ca ratio of glacial planktonic foraminifera (*G. ruber* and *G. sacculifer*) from the Caribbean and the eastern equatorial Atlantic Ocean was approximately 25% lower than Holocene values (Russell et al., 1996). Because this change was too large to be explained in terms of changes in the uranium concentration of seawater, Russell et al. (1996) hypothesized that the observed change in U/Ca ratio of planktonic foraminifera is controlled by changes in [CO_3^{2-}] or temperature.

Here we investigate the effects of changes in [CO_3^{2-}] and SST on the U/Ca in the calcite shells of planktonic foraminifera (*O. universa* and *G. bulloides*) grown in controlled laboratory cultures. We compare these results with Mg/Ca and Sr/Ca from the same culture experiments.

2. EXPERIMENTAL AND ANALYTICAL PROCEDURES

2.1. Foraminiferal Culturing Methods

Two series of culture experiments were performed at the Wrigley Institute for Environmental Studies (WIES), Santa Catalina Island, California, during the summer of 2000. Culture procedures generally followed previously established protocols (Spero and Williams, 1988; Lea et al., 1999b). Pre-sphere *O. universa* and small *G. bulloides* were collected individually by scuba divers from depths between 2–5 m in the San Pedro Basin, Southern California Bight, 2 km NNE of WIES (33°33′N, 118°30′W). Fresh seawater was collected at the dive site after each dive. At the laboratory, each specimen was measured and transferred into an acid-cleaned, sealed, 120-mL borosilicate culture jar containing filtered seawater (0.8 μm or 0.45 μm) that was modified to alter its alkalinity and [CO_3^{2-}]. Foraminifera for Experiments I and II (variable [CO_3^{2-}]) were allowed to recover for ~4 h in the culture jars at ambient temperature, and then were placed into temperature baths at 22 ± 0.1°C. Experiment III (variable temperature, ambient [CO_3^{2-}]) was conducted at 15°C, 18°C, and 25°C.

Each foraminifer was fed a single day-old *Artemia salina* nauplius (San Francisco Bay variety) (Spero et al., 1993) every other day (*G. bulloides*) or every 3 days (*O. universa*) using acid-leached borosilicate pipettes. *O. universa* was cultured under high light (300–400 μmol photons m^{-2} s^{-1}), except for one experimental group, which was cultured under low light (23 μmol photons m^{-2} s^{-1}). *G. bulloides,* a symbiont-barren species, was cultured under ambient laboratory light conditions. In culture, *G. bulloides* precipitated 1–4 chambers whereas *O. universa* secreted a large spherical chamber that accounts for ~95% of the total shell mass. Experiments ended when a foraminifer underwent gametogenesis, resulting in a shell devoid of cytoplasm. The empty shells were rinsed in distilled water and archived for analysis.

Filtered seawater was modified to obtain a range of [CO_3^{2-}] by maintaining a constant DIC and adjusting alkalinity with 1N NaOH or HCl. Under these conditions, both pH and [CO_3^{2-}] of seawater increase with alkalinity. After adding a single foraminifer to each borosilicate glass culture vessel, the seawater was topped off to eliminate the gas headspace and sealed with Parafilm and a snap top cap to prevent equilibration with atmospheric CO_2.

The modified seawater was sampled to determine the initial pH, alkalinity, and U/Ca ratio. A subset of the culture vessels from each experiment was sampled at the end of each experiment to determine the final values of these parameters. Culture solution pH was determined potentiometrically using standard NIST buffers to calibrate the pH meter. Alkalinity was determined using a Metrohm open-cell autotitrator. In some samples, DIC was measured coulometrically (Experiment II). Initial and final [CO_3^{2-}] was calculated from measured pH and alkalinity using the program of Lewis and Wallace (1998). Alkalinity, pH, and DIC measurements were calibrated against Dickson certified reference material. Experimental conditions and chemistry are reported in Table 1.

2.2. Sample Preparation and Analysis

Each foraminifer was measured and weighed before cleaning for analysis. Individual spheres of *O. universa* were cracked open using a flame-blunted glass pipette on a glass slide, and any residual juvenile calcite was removed if possible. For Experiment I, individuals from a single experimental group were sorted by weight and then were pooled in 0.6-mL microcentrifuge tubes. For Experiment II, individuals from a single experimental group were pooled, crushed, and split into replicate samples. Chambers secreted by *G. bulloides* in culture were amputated with a scalpel. All chambers grown in culture from a single experimental group were pooled to make a single analysis.

All culture samples were cleaned as follows: 1) 2 rinses with ultrapure H_2O; 2) 2–3 oxidation steps with hot buffered hydrogen peroxide (1:1 0.1 N NaOH and 30% H_2O_2) held at 70–80°C for 0.5 h for each step; 3) 5 rinses with ultrapure H_2O; 4) transfer samples to acid-leached 0.6-mL microcentrifuge tubes; 5) 1–3 rinses with 0.001 N HNO_3 (Seastar) followed by a final rinse with ultrapure H_2O. All samples from Experiments I and III were cleaned at University of California, Davis by A. Russell, and all samples from Experiment II were cleaned at University of California, Santa Barbara (UCSB) by D. Pak.

Table 1. Experimental conditions for foraminiferal culturing experiments.[a]

Experiment	Group	Light (μmol photons m^{-2} s^{-1})	T (°C)	S	Alkalinity (μequiv/kg)	pH	Mean $[CO_3^{2-}]$ (μmol/kg)	DIC (μmol/kg)	Ω_c, Ω_a
I	AR1	299–332	22	33.9	2273 ± 15	8.24 ± 0.02	213	1971–1972	5.2, 3.4
I	AR3	299–398	22	33.8	2400 ± 5	8.41 ± 0.02	301	1955–1992	7.3, 4.8
I	AR4	299–398	22	33.6	2546 ± 6	8.56 ± 0.01	399	1988	9.7, 6.3
I	AR5	299–332	22	33.6	2671 ± 23	8.66 ± 0.01	480	1990–2021	11.6, 7.8
II	BH1	23	22	33.6	2253 ± 10	8.17 ± 0.02	182	2000*	4.4, 2.9
II	BH2	365	22	33.8	2268 ± 5	8.20 ± 0.02	196	1993*	4.8, 3.1
II	BH3	332–349	22	33.7	2047 ± 15	7.74 ± 0.03	76	1965*	1.7, 1.1
II	BH4	299	22	33.7	2632 ± 12	8.65 ± 0.02	468	1979*	11.3, 7.4
II	BH5	332–365	22	33.7	2436 ± 21	8.43 ± 0.01	311	1997*	7.5, 4.9
II	BH6	299	22	33.7	2122 ± 6	7.93 ± 0.01	111	1979*	2.7, 1.7
III	AR6	332–365	15	33.8	2268 ± 12	8.22 ± 0.01	171	2016–2031	4.1, 2.6
III	AR27	332–365	18	33.7	2260 ± 8	8.17 ± 0.03	166	2001–2037	4.0, 2.6
III	AR10	282–332	25	34.2	2269 ± 15	8.21 ± 0.01	216	1936–1973	5.3, 3.5
III	AR12	282–332	25	33.7	2265 ± 6	8.21 ± 0.01	216	1949–1954	5.3, 3.5

[a] Mean $[CO_3^{2-}]$ and DIC concentrations were calculated from mean alkalinity and pH measurements using the program of Lewis and Wallace (1998), with the CO_2 constants of Mehrbach et al. (1973), refit by Dickson and Millero (1987), and K_{SO4} from Dickson (1990) ($HPO_4^- = 0.5$ μmol kg^{-1} and Si = 10 μmol kg^{-1}). Asterisks in the DIC column indicate measured values. Ω_c and Ω_a are saturation indices for calcite and aragonite, respectively.

Cleaned and crushed samples were dissolved in 0.5 mL multielement spike and were analyzed for U, Mg, Sr, and Ca using a modification of methods in Lea and Martin (1996). This method was modified to include U determination by isotope dilution using a spike of ^{235}U. Samples were analyzed using a Finnigan Element 2 high-resolution magnetic sector inductively coupled mass spectrometer (ICP-MS) at the Department of Geological Sciences (UCSB). The analytical precision (1σ) was 0.95% (Mg/Ca), 0.72% (Sr/Ca), and 3.6% (U/Ca), based on repeated analysis of a consistency standard ($n = 53$) matched in ratio and calcium concentration to the culture samples.

For the seawater samples, we used a combination of isotope dilution for U and the method of internal standards for Ca analysis. The ICP-MS was calibrated using a spiked gravimetric standard (SGS) that was prepared from a Catalina Seawater Sample (CMRC SSW11) spiked with a mixture containing enriched ^{235}U and scandium. The CMRC SSW11 sample was characterized for Ca and U using the method of standard additions before preparation of the SGS. The SGS matrix was a 22:1 dilution of the original seawater sample in 0.1% HCl. Seawater samples were spiked and diluted 22:1 with 0.1% HCl before analysis.

2.3. Data Treatment

Metal/calcium (Me/Ca) ratios for individual foraminifera cultured in this study are given in Table A1, and are accessible online (http://www.ngdc.noaa.gov/paleo/data.html). The U/Ca ratios demonstrated a bias toward higher U/Ca at sample weights less than 20 μg. Mean U/Ca ratios (Table 2) include only samples greater than 20 μg. This criterion resulted in the exclusion of 8 out of 66 analyses. One additional U/Ca analysis was excluded because it was more than 2σ greater than the mean of the remaining 5 analyses for that experimental group. Mean Mg/Ca and Sr/Ca in Table 2 exclude values that differ from the mean by more than 2σ (3 out of 66 analyses for each Me/Ca). Values excluded from the means are italicized in Table A1.

For a given $[CO_3^{2-}]$, the mean U/Ca ratios in *O. universa* shells from Experiments I and II were not significantly different. Therefore, mean U/Ca ratios for similar $[CO_3^{2-}]$ and 22°C include values from both Experiments I and II. Also, in cases for which $[CO_3^{2-}]$ concentrations calculated for Experiments I and II differed by less than 20 μmol kg^{-1}, the $[CO_3^{2-}]$ reported in Table 2 is an average of the values from Experiments I and II.

Table 2. Summary of mean (±1 S.E.) Me/Ca in cultured foraminifera.

Experiment	Species	T (°C)	$[CO_3^{2-}]$ (μmol/kg)	Mg/Ca (mmol/mol)	n*	Sr/Ca (mmol/mol)	n	U/Ca (nmol/mol)	n	$[CO_3^{2-}]$-corrected U/Ca (nmol/mol)
BH3	*O. univ*	22	76	9.41 ± 0.90	3	1.26 ± 0.05	3	15.2 ± 2.8	3	—
BH6	*O. univ*	22	111	7.92 ± 1.49	3	1.24 ± 0.06	3	10.9 ± 0.9	3	—
AR1, BH2	*O. univ*	22	205	6.82 ± 0.27	9	1.27 ± 0.01	10	9.3 ± 0.8	10	—
AR3, BH5	*O. univ*	22	306	6.68 ± 0.33	11	1.31 ± 0.01	11	7.3 ± 0.6	11	—
AR4	*O. univ*	22	399	6.42 ± 0.46	6	1.37 ± 0.02	6	6.7 ± 0.5	6	—
AR5, BH4	*O. univ*	22	474	6.49 ± 0.34	10	1.40 ± 0.01	9	4.9 ± 0.4	9	—
AR6	*O. univ*	15	171	3.53 ± 0.11	4	1.24 ± 0.01	3	9.3 ± 0.4	3	8.8 ± 0.4
AR27	*O. univ*	18	166	5.02 ± 0.33	7	1.28 ± 0.03	6	8.2 ± 0.4	6	7.7 ± 0.4
AR9–12	*O. univ*	25	216	9.60 ± 0.39	10	1.32 ± 0.02	6	9.4 ± 1.0	7	9.6 ± 1.0
BH1	*G. bull*	22	182	4.23	1	1.30	1	16.8	1	—
BH2	*G. bull*	22	196	3.82	1	1.33	1	15.3	1	—
BH3	*G. bull*	22	76	7.75	1	1.30	1	—	1	—
BH4	*G. bull*	22	468	2.69	1	1.32	1	8.1	1	—

* n refers to the number of samples included in the mean and standard error.

Table 3. Mean ($\pm 1\sigma$) concentrations of uranium and calcium in ambient seawater and culture solutions prepared from filtered seawater using unleached 0.80-μm filters and glass filter apparatus (Experiment I and II) and acid-leached polycarbonate 0.40-μm filters and Nalgene filter apparatus (Experiment III), compared with predicted values (see footnote 1 in text).

Sample	n	[Ca] (mol/kg)	[U] (nmol/kg)	U/Ca (nmol/mol)
Ambient[a]	6	0.0102 ± 0.0001	13.59 ± 0.07	1330 ± 10
Culture[a]	17	0.0102 ± 0.0001	13.60 ± 0.10	1329 ± 4
Culture[b]	17	0.0102 ± 0.0001	13.56 ± 0.09	1329 ± 7
Predicted, based on S = 33.7		0.0099	13.10	1323

[a] 0.80-μm filter.
[b] 0.40-μm filter.

We calculated shell wall thickness following the approach of Billups and Spero (1995). Our approach differed from theirs in that we subtracted 4 μg from the weight of each individual to correct for addition of gametogenic calcite (Hamilton, 1996).

3. RESULTS

3.1. U/Ca in Seawater

The concentrations of U and Ca in culture solution samples taken from the beginning and end of the experiments were the same as those in ambient seawater (±0.8%), regardless of the filter pore size (0.8 or 0.45 μm) or protocol used (Table 3). The measured [U] values were ~4% higher than those predicted using an average salinity of 33.7 p.s.u., the U/salinity relationship of Chen et al. (1986), and the Ca/salinity relationship of Millero and Sohn (1992). This difference is similar to the variability in salinity-normalized seawater [U] determined by Chen et al. (1986). These results demonstrate that the elemental U and Ca of seawater used in these culture experiments were not altered during the experiments.

3.2. Shell Me/Ca Variation with [CO_3^{2-}] or pH

In the following discussion, we report best-fit empirical relationships between shell Me/Ca and [CO_3^{2-}] or pH (Table 4a, b; Fig. 1a, b). The true theoretical form of fit depends on the mechanism driving the relationship. For example, a power function of pH would suggest that metal speciation with [CO_3^{2-}] or pH controls Me/Ca ratios, since the concentrations of U-[CO_3^{2-}] complexes vary as a power function of [CO_3^{2-}] (which in turn varies as a power function of pH). Also, the mechanisms by which changing pH influences Me/Ca may be very different from that by which changes in [CO_3^{2-}] influence Me/Ca. Relationships reported here are empirical and are meant to aid in prediction of [CO_3^{2-}] or pH from Me/Ca. They are not meant to imply a particular mechanism of incorporation.

At 22°C, shell U/Ca decreases with increasing [CO_3^{2-}] or pH in both *O. universa* (high light) and *G. bulloides* (Fig. 1a,b). The U/Ca data are best fit with an exponential function of [CO_3^{2-}], which yields $R^2 = 0.59$; $p < 0.001$ (Table 4a,b). In *G. bulloides,* an exponential relationship between U/Ca and [CO_3^{2-}] can be fit to the data (Fig. 1a), but with two fitted parameters and only three data points the relationship is suggestive at best. The preexponential constant of the *G. bulloides* curve is 40% greater than that of the *O. universa* curve. Shell U/Ca decreases by 25 ± 7% per 100 μmol kg^{-1} increase in [CO_3^{2-}] (*O. universa,* high light) and by the same magnitude (25 ± 23%) in *G. bulloides* (Table 5). Data from three individuals grown at low light indicate a significantly lower U/Ca (5.2 ± 0.5 vs. 9.3 ± 0.8 nmol mol^{-1}), but the data are too few to reach any definitive conclusion about the effect of light on U incorporation. Mg/Ca of the same individuals was equivalent within error to individuals grown at high light (6.83 ± 1.5 vs. 6.82 ± 0.27 mmol mol^{-1}), in agreement with previous work (Lea et al., 1999).

Below ambient [CO_3^{2-}], shell Mg/Ca in both species decreases with increasing [CO_3^{2-}] or pH (Fig. 1b,c; Table 4a,b). In *O. universa,* Mg/Ca decreases by 7 ± 5% per 0.1 unit increase in pH; in *G. bulloides,* Mg/Ca decreases by 16 ± 6% per 0.1 unit increase in pH. Above ambient levels, there is no significant change in Mg/Ca with increasing [CO_3^{2-}] or pH for either species. The Sr/Ca of *O. universa* shells increases by 3.3 ± 0.6% per 100 μmol kg^{-1} rise in [CO_3^{2-}], or by 1.6 ± 0.4% per 0.1 unit rise in pH above ambient levels (Fig. 1c,d; Table 4a,b). In contrast, the Sr/Ca of *G. bulloides* from our study was relatively insensitive to changes in [CO_3^{2-}] or pH; neither linear nor exponential fits were significant.

3.3. Shell Me/Ca Variation with Temperature (*O. universa*)

Between 15°C and 25°C, we observe no systematic change in *O. universa* U/Ca (Fig. 2a). Across the 10°C temperature range, the overall mean U/Ca was 9.1 ± 0.4 nmol mol^{-1} (±1 S.E., $n = 26$). Although the mean U/Ca of shells grown at 18°C (8.2 ± 0.4 nmol mol^{-1}; $n = 20$) was lower than that of shells grown at other temperatures (9.4 ± 0.5 nmol mol^{-1}; $n = 6$), this difference was not significant. Correction for slight variations in [CO_3^{2-}] due to temperature change alone did not change the trend. U/Ca in foraminiferal calcite appears to be relatively insensitive to changes in temperature compared to U/Ca in coralline aragonite, in which U/Ca decreases by 30% to 60% over a 10°C temperature increase (Min et al., 1995; Shen and Dunbar, 1995). Both Min et al. (1995) and Shen and Dunbar (1995) acknowledge the likely influence of other controls over U in corals, including [CO_3^{2-}] and salinity.

As expected, Mg/Ca in *O. universa* increased exponentially with increasing temperature, with an exponential constant of 0.096 ± 0.018 (95% confidence limit) (Fig. 2b; Table 5). Based on this relationship, the standard error of estimate for temperature was ±1.4°C. Sr/Ca ratios in *O. universa* showed a sta-

Table 4. Summary of Me/Ca relationships with $[CO_3^{2-}]$ (a), pH (b), and temperature (c) in *O. universa* (high light) and *G. bulloides* from this study.[a]

			Standard Error of Estimate	
a. Me/Ca Relationship with $[CO_3^{2-}]$	R^2	*p*	Me/Ca	$[CO_3^{2-}]$ μmol kg^{-1}
G. bulloides				
$\ln U/Ca = 3.24(\pm 0.726) - 0.0025(\pm 0.002)[CO_3^{2-}])$ $(U/Ca = 27.9 \exp(-0.0025[CO_3^{2-}])$	0.99	0.048	±0.042	±20
$Mg/Ca = 10.2(\pm 0.786) - 0.033(\pm 0.005)[CO_3^{2-}]$ $([CO_3^{2-}] \leq 200\ \mu mol\ kg^{-1})$	0.99	0.007	±0.257 mmol mol^{-1}	±100
O. universa				
$\ln U/Ca = 2.74(\pm 0.216) - 0.0025(\pm 0.0007)[CO_3^{2-}])$ $(U/Ca = 15.5 \exp(-0.0025[CO_3^{2-}])$	0.59	<0.001	±0.26	±100
$Mg/Ca = 10.8(\pm 2.60) - 0.019(\pm 0.015)[CO_3^{2-}]$, $[CO_3^{2-}] \leq 200\ \mu mol\ kg^{-1}$	0.36	0.014	±1.38 mmol mol^{-1}	±70
$Sr/Ca = 1.19(\pm 0.024) + 0.00044(\pm 7 \times 10^{-5})[CO_3^{2-}]$	0.79	<0.001	±0.028 mmol mol^{-1}	±60

b. Me/Ca Relationship with pH	R^2	*p*	Me/Ca	pH
G. bulloides				
$\ln U/Ca = 14.80(\pm 8.57) - 1.470(\pm 1.03)pH$ $(U/Ca = 2.68 \times 10^6 \exp(-1.47pH)$	0.99	0.03	±0.031	±0.02
$Mg/Ca = 73.3(\pm 24.5) - 8.47(\pm 3.05)pH$, $pH \leq 8.2$	0.99	0.02	0.086 mmol mol^{-1}	±0.01
O. universa				
$\ln U/Ca = 12.3(\pm 2.7) - 1.23(\pm 0.32)pH$ $(U/Ca = 2.20 \times 10^5 \exp(-1.23pH)$	0.59	<0.001	±0.25	±0.21
$Mg/Ca = 55.9(\pm 33.2) - 5.97(\pm 4.1)pH$, $pH \leq 8.2$	0.41	0.008	±1.33 mmol mol^{-1}	±0.22
$Sr/Ca = -0.364(\pm 0.376) + 0.201(\pm 0.045)pH$	0.67	<0.001	±0.035 mmol mol^{-1}	±0.17

c. Me/Ca Relationship with Temperature	R^2	*p*	Me/Ca	Temperature (°C)
O. universa				
$\ln Mg/Ca = -0.162(\pm 0.295) + 0.096(\pm 0.014)T$ $(Mg/Ca = 0.85 \exp(0.096{*}T))$	0.88	<0.001	0.130	±1.4
$Sr/Ca = 1.16(\pm 0.06) + 0.0056(\pm 0.003)T$	0.32	0.007	±0.03 mmol mol^{-1}	±5.4

[a] All regressions and statistics are based on individual sample analyses (not means as plotted in figures). Reported errors on slopes and intercepts are 95% confidence limits. Standard errors of estimate for linearized exponential relationships have units of ln Me/Ca; units for U/Ca are nmol mol^{-1} and units for Mg/Ca and Sr/Ca are mmol mol^{-1}. Only relationships that are statistically significant ($p < 0.05$) are included, resulting in the exclusion of Mg/Ca vs. $[CO_3^{2-}]$ (or pH) at above ambient levels ($[CO_3^{2-}] \geq 200\ \mu mol\ kg^{-1}$; $pH > 8.2$).

tistically significant increase in temperature between 15°C and 25°C, resulting in an increase of 0.4 ± 0.2% per 1°C rise in temperature (Fig. 2c; Table 4c).

4. DISCUSSION

4.1. Implications for the Incorporation of U into Calcite

The U/Ca of cleaned, pristine calcite from several species of planktonic foraminifera from core tops ranges from approximately 5 to 15 nmol mol^{-1} (~0.012–0.036 ppm) (Ku, 1965; Delaney and Boyle, 1983; Russell et al., 1994; Henderson and O'Nions, 1995; Rosenthal et al., 1999). Using an average seawater U/Ca ratio[1] of 1305 nmol mol^{-1}, these values correspond to empirical partition coefficients ($D = (U/Ca)_{shell}/(U/Ca_{sw})$ from 0.004 to 0.011, which are consistent with a partition coefficient ($D = 0.008$) obtained from culture experiments using another planktonic foraminifer, *Globigerinella calida* (Russell et al., 1994). From the present study, at ambient $[CO_3^{2-}]$ and temperature, *D* ranges from 0.007 (*O. universa*) to 0.012 (*G. bulloides*). The foraminiferal values for *D* are generally lower than laboratory-determined partition coefficients for inorganic calcite in seawater, $0.04 < D < 0.26$ (Kitano and Oomori, 1971) and $0.046 < D < 0.2$ (Meece and Benninger, 1993). At face value, this suggests a biologic control over the incorporation of U into foraminiferal calcite. Biologic discrimination also appears to affect Mg in calcite shells of foraminifera, for which *D* (~0.002 at 25°C, this study) is at least an order of magnitude lower than the inorganic *D* at the same temperature, 0.017 (Mucci, 1987) to 0.057 (Katz, 1973). However, caution must be used in comparing distribution coefficients for U in inorganic calcite with foraminiferal U partition coefficients. This is because inorganic calcite precipitation experiments by both Kitano and Oomori (1971) and Meece and Benninger (1993) were performed using seawater [U] at least 100 times greater than that present in the surface ocean. U incorporation into calcite under such extreme conditions is unlikely to resemble incorporation under natural conditions.

The incorporation of trace elements into minerals involves processes occurring within the fluid (aqueous speciation, dif-

---

[1] Based on average salinity-normalized $[U] = 13.60$ nmol kg^{-1} (Chen et al., 1986) and $[Ca] = 10.28$ mmol kg^{-1} (Millero and Sohn, 1992).

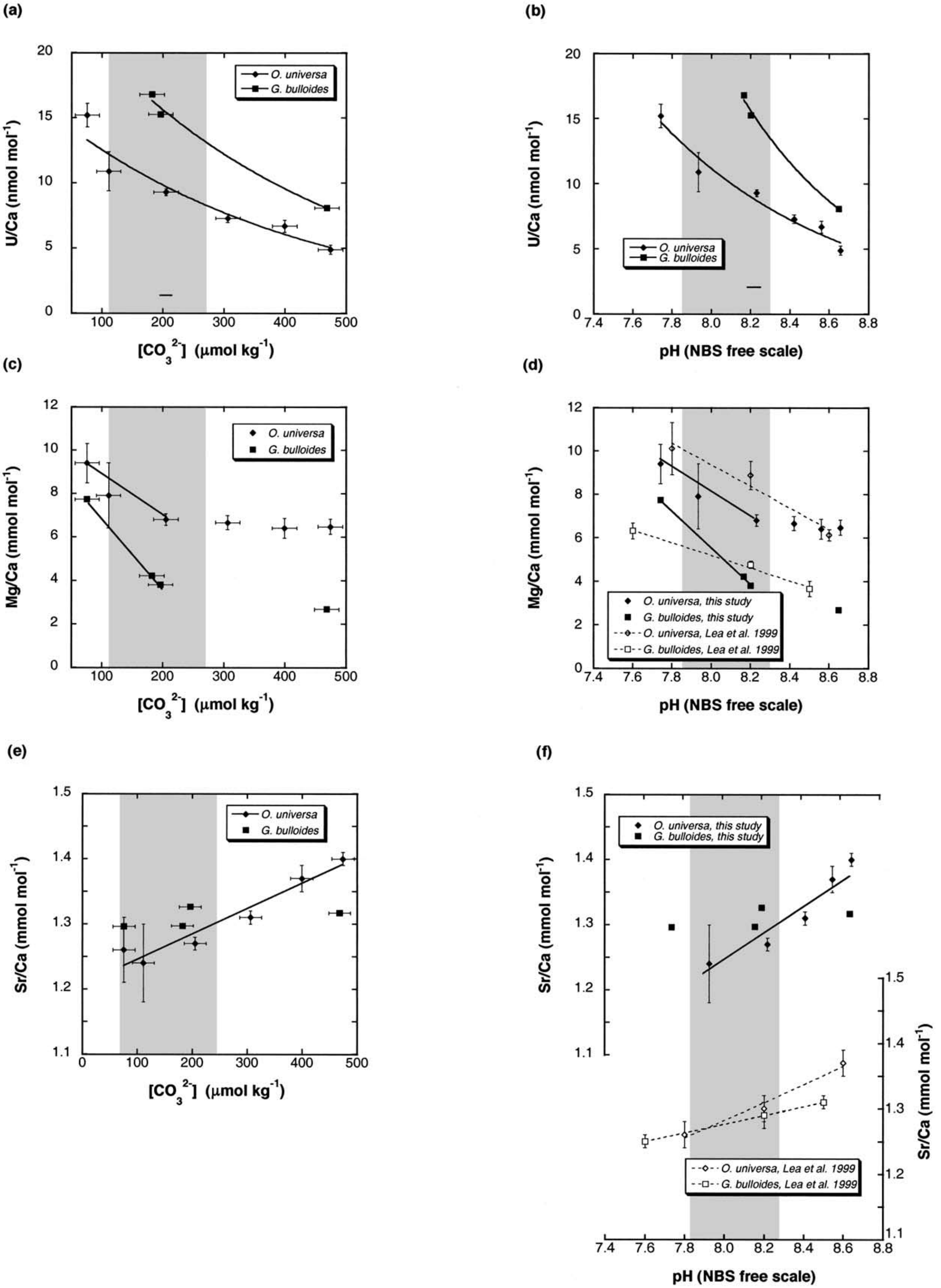

Fig. 1. Dependence of shell U/Ca, Mg/Ca, and Sr/Ca of *O. universa* (high light) and *G. bulloides* on seawater $[\mathrm{CO}_{>3}^{2-}]$ (a, c, e) or pH (b, d, f). Shaded areas show the range of $[\mathrm{CO}_3^{2-}]$ or pH in the modern surface ocean (Bainbridge et al., 1981; Chen, 1984). The horizontal bar in (a) and (b) shows the range of ambient $[\mathrm{CO}_3^{2-}]$ or pH in our experiments. Data from Lea et al. (1999) are shown for comparison in (d) and (f). Regression parameters for this and subsequent plots are based on regression through individual analyses (not means as plotted). Error bars are ±1 standard error. *O. universa* points are means of 3 to 11 individual analyses of pooled shells; *G. bulloides* points are single analyses of multiple pooled chambers. See Tables 4 and 5 for regression equations and Me/Ca responses (as %) to changes in $[\mathrm{CO}_3^{2-}]$ and pH.

Table 5. Summary of Me/Ca responses (as %) to changes in seawater $[CO_3^{2-}]$, pH, and temperature.[a]

Species	Percent change in Me/Ca in response to change of: +100 μmol kg^{-1} in $[CO_3^{2-}]$	+0.1 unit in pH	+1°C in Temperature
U/Ca			
G. bulloides	−25 ± 23	−15 ± 10	—
O. universa	−25 ± 7	−12 ± 3	—
Mg/Ca			
G. bulloides	−63 ± 9	−16 ± 6	—
O. universa	−23 ± 18	−7.2 ± 4.9	+9.6 ± 1.4
Sr/Ca			
G. bulloides	—	—	—
O. universa	+3.3 ± 0.6	+1.6 ± 0.4	+0.4 ± 0.2

[a] Responses are calculated from the exponential constants for exponential fits and from the slope divided by the mean Me/Ca for linear fits. Responses for Mg/Ca to changes in $[CO_3^{2-}]$ and pH are for $[CO_3^{2-}] \leq 200$ μmol kg^{-1} and pH ≤ 8.2.

fusion), on the mineral surface (adsorption and desorption, ligand exchange reactions, rearrangement of ligand coordination), and within the solid (coordination changes, solid diffusion). The concentration of carbonate ion may influence the incorporation of uranium into calcium carbonate through one or a combination of these processes.

Uranium exists in seawater almost exclusively as a group of carbonate complexes (Djogic et al., 1986) in which one to three carbonate groups are attached equatorially to a central linear uranyl ion (Clark et al., 1995). The relative abundance of each complex depends on $[CO_3^{2-}]$, by the following reactions[2]:

$$UO_2^{2+} + CO_3^{2-} \Leftrightarrow UO_2CO_3^{\circ} \qquad \log \beta 1 = 8.46$$

$$UO_2CO_3^{\circ} + CO_3^{2-} \Leftrightarrow UO_2(CO_3)_2^{2-} \qquad \log \beta 2 = 15.65$$

$$UO_2(CO_3)_2^{2-} + CO_3^{2-} \Leftrightarrow UO_2(CO_3)_3^{4-} \qquad \log \beta 3 = 21.76$$

The triscarbonato complex ($UO_2(CO_3)_3^{4-}$) is the predominant uranium species at the range of pH in seawater, accounting for >99% of total uranium. In this species, the three CO_3^{2-} moieties are attached bidentally via two O atoms to the central U ion in the equatorial plane (Clark et al., 1995). The predominance of uranyl carbonate complexes in seawater led to the suggestion that U substitutes as a uranyl carbonate complex into coral aragonite, replacing one or more CO_3 or $CaCO_3$ groups, rather than substituting as the divalent cation UO_2^{2+} for Ca^{2+} (Swart and Hubbard, 1982). Using X-ray absorbance, luminescence, and Raman spectroscopy, Reeder et al. (2000) showed that in aragonite, U maintains the same coordination (CN = 6) and geometry as in the dissolved uranyl triscarbonato complex, and is most likely incorporated directly as $UO_2(CO_3)_3^{4-}$, replacing Ca and some CO_3 groups. In calcite, however, U coordination differs, reflecting some monodentate CO_3 groups and a greater degree of disorder than in aragonite. Reeder et al. (2000) suggest that the change in coordination required to incorporate U into calcite may explain its relative paucity compared to U in aragonite, for which no coordination change is necessary. Alternatively, it is possible that because of the coordination changes required to incorporate $UO_2(CO_3)_3^{4-}$ into calcite, one or more of the less abundant species are incorporated instead. Since the abundance of $UO_2CO_3^{\circ}$ and $UO_2(CO_3)_2^{2-}$ decreases with increasing carbonate concentration, incorporation of either or both in preference to $UO_2(CO_3)_3^{4-}$ is

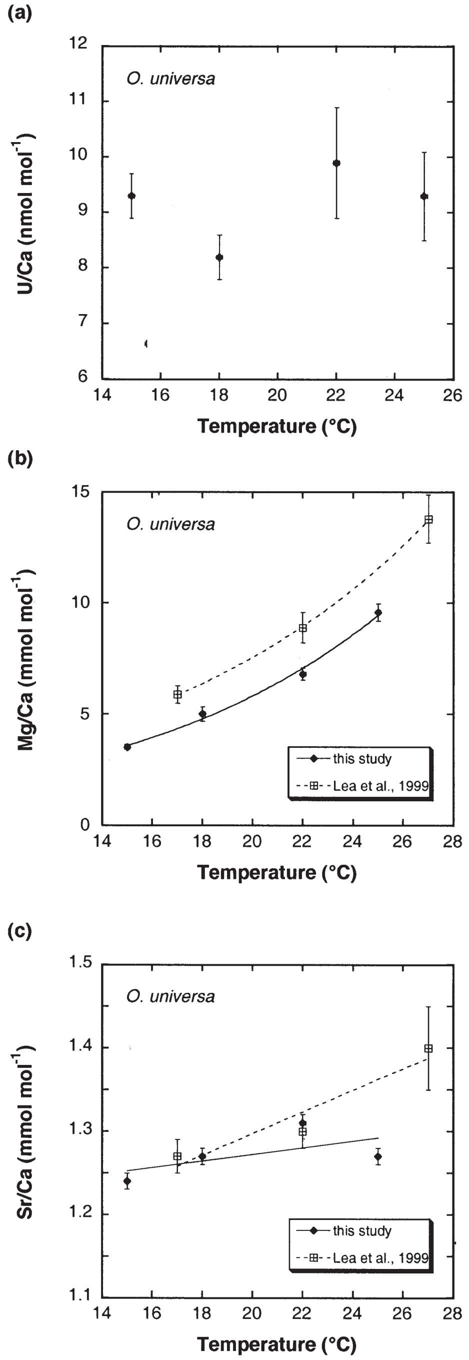

Fig. 2. Dependence of shell U/Ca (a), Mg/Ca (b), and Sr/Ca (c) of *O. universa* (high light) on seawater temperature, under ambient $[CO_3^{2-}]$. Each data point represents a mean of 4 to 10 individual analyses of pooled shells. Data from Lea et al. (1999) are shown for comparison in (b) and (c). See Tables 4 and 5 for regression equations and Me/Ca responses (as % per °C) to temperature change.

---

[2] Constants are adjusted to an ionic strength of 0.7, using the specific ion activity approach (Grenthe et al., 1992).

consistent with the inverse relationship between U/Ca and [CO_3^{2-}] observed in our culture experiments.

The offset between higher U/Ca in *G. bulloides* and relatively low U/Ca in *O. universa* (at the same bulk solution [CO_3^{2-}]) is qualitatively consistent with a change in U speciation near the shell wall of the symbiont-bearing *O. universa*. Photosynthesis by algal symbionts associated with *O. universa* consumes CO_2, thereby increasing pH at the calcifying shell wall by ~0.5 pH units under high light conditions. Similarly, respiration produces CO_2, thereby reducing pH at the shell wall by ~0.4 pH units relative to ambient conditions (Rink et al., 1998). Since *G. bulloides* has no symbionts, pH (and [CO_3^{2-}]) at the shell wall must be lower than pH at the calcifying surface of *O. universa*. The higher U/Ca observed for *G. bulloides* relative to *O. universa* (Fig. 1a) is consistent with this hypothesis. A similar offset was observed between boron isotopes ($\delta^{11}B$) in *G. bulloides* and *O. universa*. In this case, the $\delta^{11}B$ of *G. bulloides* from plankton tows was 1.4‰ lower than that of *O. universa,* consistent with *G. bulloides* calcifying at a lower microenvironment pH compared to *O. universa* (Hönisch et al., 2003).

Surface processes involved in trace metal incorporation into calcite, such as sorption-desorption and surface structural controls, might also be affected by changes in [CO_3^{2-}]. Adsorption of uranium onto different mineral and organic surfaces such as clays, ferric oxyhydroxides, hydrous titanium oxides, and humic acids is inhibited as pH and [CO_3^{2-}] increase. This is most likely due to the strong tendency of uranyl ion to form dissolved carbonate complexes (Langmuir, 1978; Ames et al., 1983; Hsi and Langmuir, 1985; Tamon et al., 1990; Barnett et al., 2000). Because adsorption of U precedes incorporation into the mineral structure, increased carbonate concentrations should lower overall U incorporation, as observed in our experiments.

In the last decade, a number of studies have revealed the importance of surface structural controls within calcite growth sectors over the incorporation of divalent cations such as Mg, Co, Zn, Mn, Cd, Sr, Ba, and Pb (Paquette and Reeder, 1995; Reeder, 1996) and anions (SO_4^{2-}, SeO_4^{2-}, and B and U oxyanions) (Staudt et al., 1994; Hemming et al., 1998; Reeder et al., 2000; Reeder et al., 2001). Reeder et al. (2001) demonstrated that U is distributed inhomogeneously between nonequivalent vicinal faces of spiral growth hillocks within the dominant 1014 calcite. U concentrations are enriched by a factor of 6 to 10 on a′ and b′ vicinal faces compared to a and b faces. This pattern is similar to that observed for Mg (Paquette and Reeder, 1995) and B (Hemming et al. 1998), and opposite to the pattern observed for Sr (Paquette and Reeder, 1995). The relative growth rate of these pairs of nonequivalent faces is a function of the solution Ca^{2+}/CO_3^{2-} concentration ratio (Gratz et al., 1993; Paquette and Reeder, 1995; Reeder, 1996). On a growing crystal, relatively rapid growth occurs on *a* and *b* faces compared to a′ and b′ faces. If these observations can be extrapolated to bulk calcite, calcite formed in high-[CO_3^{2-}] waters should contain a larger fraction of *a′* faces compared to that formed in low-[CO_3^{2-}] waters. Because the U content of *a′* faces is relatively high, U in bulk calcite should increase with solution [CO_3^{2-}]. This is opposite to the inverse trend that we observed between shell U/Ca and solution [CO_3^{2-}], suggesting that surface structural controls of this nature are not a dominant influence on U incorporation into planktonic foraminiferal calcite.

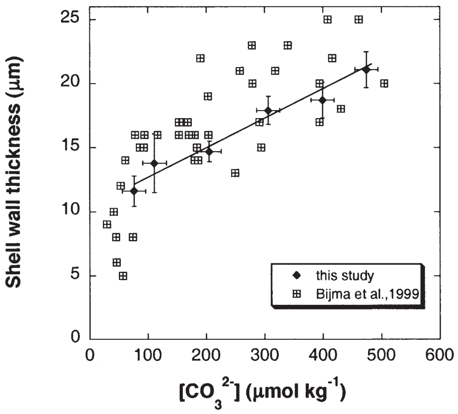

Fig. 3. Dependence of *O. universa* shell wall thickness on seawater [CO_3^{2-}] from the current study, compared with wall thickness calculated from data in Bijma et al. (1999). Shell wall thickness is calculated from final shell radius and weight, assuming constant 12% porosity and subtracting 4 μg gametogenic calcite per individual.

Calcification rate may also play an important role in the incorporation of metals into carbonates. The distribution coefficient of Sr increases with calcification rate in both inorganically precipitated calcite (Lorens, 1981; Morse and Bender, 1990) and in biogenic calcite from coccolithophorids (Stoll et al., 2002). The observed increase of Sr/Ca in *O. universa* with [CO_3^{2-}] in our experiments is consistent with a calcification rate control over Sr/Ca. In contrast, Mg incorporation into inorganic calcite appears to be unaffected by calcification rate over a range of saturation states (Mucci and Morse, 1983; Mucci et al., 1985).

Previous studies have shown that shell weights of cultured *O. universa* increase with [CO_3^{2-}], with a steeper rate of increase at [CO_3^{2-}] below modern ambient levels (Bijma et al., 1999). In our experiments, the wall thickness of *O. universa* individuals increased with [CO_3^{2-}] (Fig. 3). The relationship between shell wall thickness and [CO_3^{2-}] from our study is the same as that based on the Bijma et al. (1999) data set (also shown in Fig. 3). If we can assume that cultured foraminifera added calcite in the same manner in each experiment, this increase in wall thickness suggests a calcification rate increase with higher [CO_3^{2-}].

The inverse relationship between foraminiferal U/Ca and [CO_3^{2-}] could be related to calcification rate in two ways. First, U incorporation could be enhanced at slow calcification rates because the bulky uranyl carbonate complex is allowed time to adjust sterically to fit into the calcite matrix. Alternatively, higher [CO_3^{2-}] could increase the proportion of calcite precipitated at night, when low pH conditions created by addition of respiratory CO_2 are not offset by higher pH created by symbiont photosynthesis. This explanation would suggest that light levels could influence U incorporation in symbiont-bearing foraminifera species, and is consistent with an offset toward higher U in non-symbiont-bearing species. However, the U/Ca of shells from the single low-light *O. universa* experimental group (5.2 ± 0.5 nmol mol^{-1}), cultured at ambient temperature and [CO_3^{2-}], is significantly lower than shells from the high light ambient group (9.3 ± 0.8 nmol mol^{-1}). Because the effects of symbiont photosynthesis are nil under low light conditions, we would expect the U/Ca of these shells to be *higher* than that of the high light ambient group. The effects of light on foraminiferal U/Ca must be clarified in further experiments.

The lack of increase in shell Mg/Ca with increasing $[\mathrm{CO_3^{2-}}]$ suggests that precipitation of inorganic calcium carbonate from solution onto shells did not affect our experiments. Because partition coefficients for Mg in inorganic calcite at 25°C are at least an order of magnitude greater than foraminiferal partition coefficients (Katz, 1973; Mucci, 1987), we would expect an increase in Mg/Ca with increasing $[\mathrm{CO_3^{2-}}]$ if precipitation of inorganic calcium carbonate were significant in these experiments. Such an increase was not observed.

4.2. Potential for Foraminiferal U/Ca as an Indicator of Past Changes in Seawater $[\mathrm{CO_3^{2-}}]$

We evaluate the utility of foraminiferal U/Ca as an indicator of changes in surface-water $[\mathrm{CO_3^{2-}}]$ by calculating $[\mathrm{CO_3^{2-}}]$ based on U/Ca records from one Caribbean core (CP6001-4; 14°55′N, 71°50′W, 3645 m) and an eastern equatorial Atlantic core (EN066-17GGC; 5°22′N, 21°5′W, 3050 m (Fig. 4; replotted from Russell et al., 1996). We also consider data from another nearby equatorial Atlantic core (EN066-39GGC; 5°4′N, 20°52′W, 2818 m). Core processing, analytical methods, and age estimates for U/Ca records from CP6001-6 and EN066-17GGC are reported in Russell et al. (1996). We compare estimates of Holocene surface-water $[\mathrm{CO_3^{2-}}]$ in the Caribbean Sea and the eastern equatorial Atlantic Ocean with $[\mathrm{CO_3^{2-}}]$ computed from Holocene U/Ca in *G. sacculifer* from these cores. Finally, we compare the average glacial-Holocene differences in U/Ca-based $[\mathrm{CO_3^{2-}}]$ in these cores (Table 6) with theoretical estimates as well as estimates based on data from other carbonate system proxies.

Because diagenetic alteration of the primary U/Ca signal can arise as a result of partial dissolution of foraminiferal shells (Russell et al., 1994) and/or authigenic overgrowths of manganous carbonate (Boyle, 1983), we first evaluate the potential impact of diagenesis on the U/Ca signal from the three cores chosen. The constancy of foraminiferal fragmentation in EN066-17GGC between marine isotope stages 1 and 2 (6 and 7%, respectively; Curry and Lohmann, 1986) suggests that down-core U/Ca changes in this core and in the shallower core EN066-39GGC are not likely to be due to partial dissolution. Dissolution is also unlikely in the glacial portion of CP6001-4 where aragonitic pteropods are found, indicating excellent calcite preservation. Foraminiferal fragmentation in CP6001-4 is less than 10% through MIS 6, suggesting minimal dissolution. In addition, Holocene (4.5–10.5 kyr) SST based on Mg/Ca in *G. sacculifer* from CP6001-4 (Russell et al., 1996) was 25.9 ± 0.8°C[3], consistent with annual mean observed temperatures at 50–75 m (14.5°N, 70.5°W) (http://iridl.ldeo.columbia.edu/SOURCES/.LEVITUS94/.ANNUAL/.temp). The calculated Holocene temperatures are consistent with minimal shell dissolution, since *G. sacculifer* dwells in the mixed layer and adds gametogenic calcite at depth.

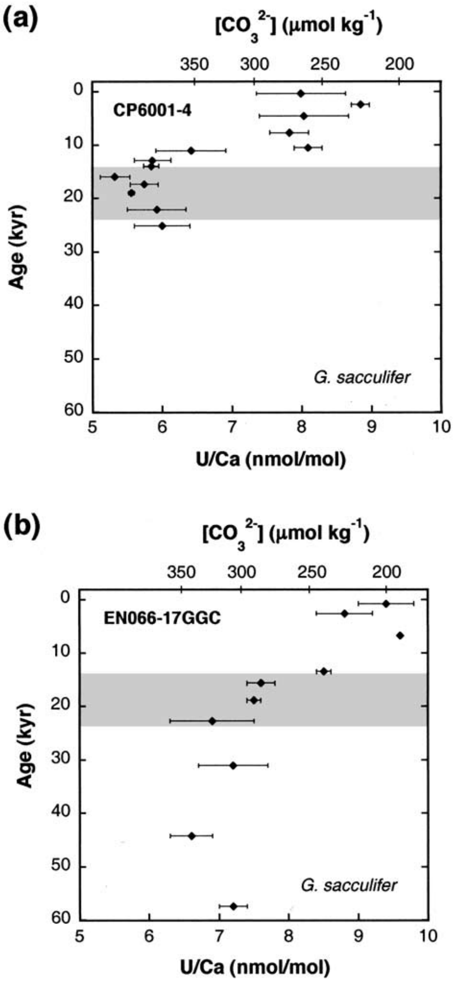

Fig. 4. Profiles of U/Ca in *G. sacculifer* vs. age for (a) CP6001-4 (Caribbean) and (b) EN066-17GGC (eastern equatorial Atlantic), replotted from Russell et al. (1996). Shaded area represents MIS 2. The $[\mathrm{CO_3^{2-}}]$ scale is based on the *O. universa* U/Ca-$[\mathrm{CO_3^{2-}}]$ exponential relationship from our experiments (Table 4). U/Ca ratios in EN066-17GGC are ~1.4 nmol mol^{-1} higher than in nearby core EN066-39GGC (Rosenthal, unpublished data) and probably underestimate absolute $[\mathrm{CO_3^{2-}}]$ (see text); however, the glacial/Holocene difference in U/Ca (and $[\mathrm{CO_3^{2-}}]$) is the same in both EN066-17GGC and EN066-39GGC (Table 6).

The correlation between U/Ca and Mn/Ca in many cores (P. Martin and D. Lea, unpublished data) suggests that foraminiferal U/Ca may be strongly affected by U incorporation into these secondary carbonates. However, because there is no positive correlation observed between U/Ca and Mn/Ca in the sections of cores discussed here (Russell et al., 1996; Rosenthal, unpublished data), it is unlikely that the U/Ca signal in these intervals is controlled by Mn overgrowths.

We estimated Holocene surface-water $[\mathrm{CO_3^{2-}}]$ from modern temperature, salinity, and alkalinity data[4] from WOCE transects A22 (western Atlantic/Caribbean) and A06 (eastern equatorial

---

[3] Calculated using Dekens et al. (2002) core top calibration for *G. sacculifer,* at water depth of 20 m (Mg/Ca = 0.37exp(0.09T)).

[4] For the Caribbean, we averaged temperature, salinity, and alkalinity data from the upper 10 dbar from WOCE section A22 between station 1 (11°N) and station 35 (19°N) along 66°W, and assumed equilibrium with atmospheric $p\mathrm{CO_2} = 275$ μatm. Thus, T = 28.2°C, S = 35.9 PSU, and alkalinity = 2349 μequiv/kg (http://cdiac.esd.ornl.gov/oceans/woce_a22.html).

Atlantic) in combination with the average pCO_2 over the last 7 kyr (275 μatm) from the Taylor Dome (Antarctica) ice core record (Brook et al., 1999; Indermühle et al., 1999). For the Caribbean, we assumed equilibrium between atmospheric and surface water pCO_2, whereas for the eastern equatorial Atlantic Ocean, we assumed that the average modern sea-air offset of 17 μatm (http://ingrid.ldeo.columbia.edu/SOURCES/.LDEO/.Takahashi/) has not changed. With these assumptions, the Holocene surface water $[CO_3^{2-}]$ is 290 μmol kg^{-1} in the Caribbean and 275 μmol kg^{-1} in the eastern equatorial Atlantic Ocean.

Using the average (±1σ) U/Ca in *G. sacculifer* (355–425 μm) from Holocene intervals of CP6001-4, 7.9 ± 0.8 nmol mol^{-1}, we calculate an average Holocene surface-water $[CO_3^{2-}]$ in the Caribbean of 280 ± 50 μmol kg^{-1}, in agreement with the value based on water and ice data. The average Holocene (MIS I) U/Ca in *G. sacculifer* from EN066-39GGC (7.9 ± 0.8 nmol mol^{-1}) (Rosenthal, unpublished data) is the same as that in the Caribbean core, yielding a Holocene U-based $[CO_3^{2-}]$ of 280 ± 40 μmol kg^{-1}, again in agreement with values estimated from water and ice core data. Holocene U/Ca in EN066-39GGC is significantly lower than the ratio from nearby EN066-17GGC, U/Ca = 9.3 ± 0.4 nmol mol^{-1} (Russell et al., 1996). This offset is systematic through the core, and probably arises from differences in cleaning methods. The most significant methodological difference is that the initial sample weights from EN066-17GGC (~3.5 mg) were much larger than those from EN066-39GGC (100–200 μg), due to analytical requirements. The efficiency of removing clays, organic matter, and manganese overgrowths is likely to be greater for smaller samples. It should also be noted that significant inter-laboratory offsets may exist for U in foraminifera, as have been observed for Mg (which is much more abundant in foraminifera than U). A recent inter-calibration study showed that inter-laboratory variability for Mg in cleaned foraminifera was ±8% (%RSD), whereas variability in standard solutions was only ±1.5%. This variability was attributed to differences in cleaning methods (Rosenthal et al., 2004).

Average U/Ca for the glacial intervals of CP6001-4 was 6.0 ± 0.7 nmol mol^{-1}, corresponding to a glacial $[CO_3^{2-}]$ of 390 ± 50 μmol kg^{-1}, or a glacial–interglacial difference ($\Delta[CO_3^{2-}]$) of 110 ± 70 μmol kg^{-1}. In EN066-39GGC, average glacial U/Ca was 6.3 ± 0.1 nmol mol^{-1} ($[CO_3^{2-}]$ = 360 ± 10 μmol kg^{-1}) or $\Delta[CO_3^{2-}]$ = 80 ± 40 μmol kg^{-1}. This difference is identical to the glacial–Holocene difference determined from EN066-17GGC (Russell et al., 1994).

These $\Delta[CO_3^{2-}]$ estimates are consistent with estimates of glacial–interglacial $[CO_3^{2-}]$ change in surface waters (Lea et al., 1999a). Based on assuming equilibrium at 25°C between the surface ocean and atmospheric pCO_2 = 200 μatm, estimated $\Delta[CO_3^{2-}]$ in surface waters range from 50 μmol kg^{-1} (extraction of CO_2 via the biologic pump) to 120 μmol kg^{-1} (addition of alkalinity from $CaCO_3$ dissolution) (Lea et al., 1999a). In the northwestern African upwelling zone, glacial pH estimates from boron isotope data suggest that glacial surface ocean $[CO_3^{2-}]$ may have been ~70 to 100 μmol kg^{-1} higher than interglacial levels. This estimate is based on a 0.2 pH unit increase in surface water pH and assumes either a change in total CO_2 by nutrient depletion or a 2:1 change in alkalinity and total CO_2 by carbonate addition during the glacial period (Sanyal and Bijma, 1999). In the North Atlantic, changes in foraminiferal weights suggest that glacial surface-water $[CO_3^{2-}]$ was ~80 μmol kg^{-1} higher than Holocene values (Barker and Elderfield, 2002).

4.3. Implications of Mg/Ca and Sr/Ca Results

The relationships between shell Mg/Ca and Sr/Ca and $[CO_3^{2-}]$ (pH) and temperature obtained from our results differ somewhat from experimental results obtained previously (Lea et al., 1999b). For *O. universa,* we believe that the results of the current study are likely to be more reliable. First, the current study included more experimental data points (six $[CO_3^{2-}]$ values and four temperatures, compared to three $[CO_3^{2-}]$ values and three temperatures tested in the Lea et al. (1999b) study). Secondly, the current study used improved cleaning techniques to remove organic matter from the foraminifera. Samples from the Lea et al. (1999b) experiments were cleaned using 5% sodium hypochlorite (bleach), whereas we used buffered 30% hydrogen peroxide in this study. Results of cleaning experiments by D. Pak (UCSB, unpublished data) suggest that H_2O_2 is more effective than NaClO at oxidizing organic matter in recently dead foraminifera. Finally, measurement precision, estimated at ~2% for Mg/Ca and ~1% for Sr/Ca in Lea et al. (1999b), is significantly better for both Mg/Ca (0.9%) and Sr/Ca (0.8%) in this study.

In the Lea et al. (1999) study, Mg/Ca in *O. universa* and *G. bulloides* both decreased by ~6% per 0.1 unit increase in pH over the pH range examined (pH 7.6 to 8.6). Our results show a similar dependence below ambient pH in *O. universa* (−7% per 0.1 pH unit), but a significantly larger response below ambient pH in *G. bulloides* (−16% per 0.1 pH unit). In both species, the dependence of Mg/Ca on pH was insignificant at pH greater than 8.2.

The record of pCO_2 in the Vostok ice core suggests that surface ocean pH has not been lower than modern values for most of the last 420 kyr (Lea et al., 1999a; Petit et al., 1999). Since Mg/Ca appears to be insensitive to pH at values higher than modern, Mg/Ca-based paleotemperatures over the past 420 kyr are probably not biased significantly by variations in surface water pH. However, temperature reconstructions based on planktonic foraminiferal Mg/Ca for periods during which surface ocean pH was lower than modern, such as during the Cretaceous (Zeebe, 2001), should correct for variations in pH. Because neither a symbiotic species (*O. universa*) nor a non-symbiotic species (*G. bulloides*) display any significant Mg/Ca relationship with pH across oceanic values considered relevant for Quaternary paleoceanography, we suggest that these observations could be a general aspect of Mg incorporation in planktonic foraminifera. Given the different pH dependencies observed for these two species, however, it is not possible to predict the actual Mg/Ca dependence on pH for other species without further experimental research.

Compared to the relationship reported in Lea et al. (1999), the Mg/Ca-T relationship for *O. universa* presented here has the same exponential constant (within error) between T and Mg/Ca (0.096 ± 0.014 vs. 0.085 ± 0.022), but it has a lower preexponential constant ($0.85^{+0.30}_{-0.22}$ mmol mol^{-1}) than the original relationship in Lea et al. (1999) ($1.36^{+0.84}_{-0.52}$ mmol mol^{-1}). The current data provide a firmer basis for an exponential fit, because the new relationship is based on four temperatures

Table 6. Average ($\pm 1\sigma$) Holocene U/Ca in *G. sacculifer* and $[CO_3^{2-}]$ estimated from U/Ca in Atlantic and Caribbean cores, compared to $[CO_3^{2-}]$ calculated from WOCE measurements (a); and average ($\pm 1\sigma$) glacial U/Ca and $[CO_3^{2-}]$ and glacial–interglacial $\Delta[CO_3^{2-}]$ (b). Errors in G-IG $\Delta[CO_3^{2-}]$ are propagated from the variance of Holocene and glacial U/Ca.

(a)	Holocene				
Core	Interval (kyr)	*n*	U/Ca (nmol mol^{-1})	Estimated $[CO_3^{2-}]$ (μmol kg^{-1})	WOCE $[CO_3^{2-}]$ (μmol kg^{-1})
CP6001-4	0.3–11	18	7.9 ± 0.8	280 ± 50	290
EN066-17GGC	0–7	9	9.3 ± 0.2	210 ± 20	275
EN066-39GGC	0–11	5	7.9 ± 0.8	280 ± 40	275

(b)	Glacial				
Core	Interval (kyr)	*n*	U/Ca (nmol mol^{-1})	Estimated $[CO_3^{2-}]$ (μmol kg^{-1})	Estimated G-IG $\Delta[CO_3^{2-}]$ (μmol kg^{-1})
CP6001-4	14–22	16	6.0 ± 0.7	390 ± 50	110 ± 70
EN066-17GGC	13–23	11	7.7 ± 0.2	290 ± 30	80 ± 40
EN066-39GGC	14–25	5	6.3 ± 0.1	360 ± 10	80 ± 40

rather than three as previously tested. The lower preexponential constant in the present study is probably due to improvements in cleaning techniques. Both sets of culture experiments produced higher preexponential constants than determined for *O. universa* by Anand et al. (2003) (0.595 ± 0.04 mmol mol^{-1}) from Sargasso Sea sediment trap samples. The reason for the difference between sediment trap and culture experiments is not obvious, but it is clear from the sediment trap data that *O. universa* Mg/Ca does not follow a simple seasonal pattern, as observed for surface dwelling planktonic foraminifera (Anand et al., 2003).

The relationship between Sr/Ca and pH (or $[CO_3^{2-}]$) in *O. universa* is similar to or slightly greater than previously reported (1.6 ± 0.4% vs. 1.1 ± 0.5% change per 0.1 pH unit), whereas the relative insensitivity of Sr/Ca to pH in *G. bulloides* agrees with earlier results (Lea et al., 1999b). This species difference in response to $[CO_3^{2-}]$ may be due to interspecies differences in surface structural controls over calcification (e.g., Paquette and Reeder, 1995), or possibly to an influence over calcification rate exerted by photosynthetic symbionts in *O. universa*. If the Sr/Ca-pH relationship for other symbiont-bearing planktonic species is similar to that of *O. universa,* caution should be exercised in interpreting Sr/Ca records from such species in terms of changes in seawater Sr/Ca because of the possible confounding effects of variable $[CO_3^{2-}]$ (e.g., Stoll et al., 1999).

The Sr/Ca dependence on temperature (0.4 ± 0.2% per degree for *O. universa*) is smaller than the previously observed value of ~0.9% per degree for both species (Lea et al., 1999b). If the dependence derived from the present study is more representative, it suggests that temperature can only account for a small part of the observed downcore variation in Sr/Ca (Martin et al., 1999).

5. CONCLUSIONS

Results from culture experiments demonstrate that shell U/Ca ratios in *O. universa* decrease exponentially with increasing seawater $[CO_3^{2-}]$, with a U/Ca decrease of 22% per 100 μmol kg^{-1} increase in $[CO_3^{2-}]$. In *G. bulloides,* U/Ca also declined as $[CO_3^{2-}]$ increased, but the preexponential constant of this curve was 40% greater than that of *O. universa*. The decrease in U/Ca with increasing $[CO_3^{2-}]$ is qualitatively consistent with incorporation of mono- or bi-carbonate uranyl complexes, or with reduced U adsorption at higher $[CO_3^{2-}]$. We did not observe a consistent change in U/Ca of *O. universa* with temperature between 15°C and 25°C.

Using the U/Ca-$[CO_3^{2-}]$ relationship and records of U/Ca in *G. sacculifer* from eastern equatorial Atlantic Ocean cores, we estimate that $[CO_3^{2-}]$ in glacial surface waters was 80 ± 40 μmol kg^{-1} higher than during the Holocene. In the Caribbean, this change was 110 ± 70 μmol kg^{-1}. This change in surface-water $[CO_3^{2-}]$ agrees well with the change estimated from elevated glacial pH based on boron isotopes in the eastern equatorial Atlantic upwelling zone (100 μmol kg^{-1}) (Sanyal and Bijma, 1999), and an estimate of ~80 μmol kg^{-1} increase in North Atlantic surface waters based on foraminiferal weights (Barker and Elderfield, 2002). These results suggest that, in settings where the addition of U by diagenetic processes is not a factor, downcore records of foraminiferal U/Ca have potential to provide information about changes in the ocean's carbonate concentration. Because manganous carbonate overgrowths occur in reducing sediments (where dissolved Mn^{2+} appears in pore fluids) that are overlain by oxic bottom waters, this technique is most likely to be successful in well-oxygenated sediments.

Below ambient pH (pH = 8.2), Mg/Ca decreased by 7 ± 5% (*O. universa*) to 16 ± 6% (*G. bulloides*) per 0.1 unit increase in pH. In both species, the change in Mg/Ca at pH above ambient was insignificant. These results imply that paleotemperatures computed from foraminiferal Mg/Ca during the late Quaternary have not been influenced significantly by variations in ocean pH. As expected, shell Mg/Ca increased exponentially with temperature in *O. universa* in our experiments, with a lower preexponential constant than observed in earlier culture studies by Lea et al. (1999). The Mg/Ca temperature dependence of 9.6 ± 1.4% per °C for *O. universa* agrees well with the range of 8–11% reported for other planktonic species (Mashiotta et al., 1999; Dekens et al., 2002; Anand et al., 2003).

In *O. universa,* Sr/Ca increased linearly by 3.3 ± 0.6% per 100 μmol kg^{-1} increase in [CO_3^{2-}] (or 1.6 ± 0.4% per 0.1 unit increase in pH); a larger increase than observed in the earlier experiments. In contrast, Sr/Ca of *G. bulloides* shells was independent of [CO_3^{2-}], in agreement with earlier results. The change of Sr/Ca in *O. universa* with temperature was weak (0.4 ± 0.2% per 1°C).

Acknowledgments—We thank L. Juranek, M. Thomas, and H. Iverson for assistance with the culture experiments, D. Pak for cleaning foraminifera at UCSB, and G. Paradis (UCSB) for the ICP-MS analyses. Y. Rosenthal generously contributed his data from EN066-39GGC. The paper benefited from two anonymous reviews and from discussions with M. Schmidt. This research was funded by NSF grants OCE-9907044 (A.D.R.), OCE-9729203 (H.J.S.), OCE-0117886 (D.W.L.), and OCE-9986716 (Y.R.).

Associate editor: T. Shaw

REFERENCES

Ames L., McGarrah J., and Walker B. (1983) Sorption of uranium and radium by biotite, muscovite, and phlogopite. *Clay and Clay Min* **31,** 343–351.

Anand J., Elderfield H., and Conte M. (2003) Calibration of Mg/Ca thermometry in planktonic foraminifera from a sediment trap time series. *Paleoceanography* **18,** 1050, 10.1029/2002PA000846.

Archer D., and Maier-Reimer E. (1994) Effect of deep-sea sedimentary calcite preservation on atmospheric CO_2 concentration. *Nature* **367,** 260–263.

Archer D., Winguth A., Lea D. W., and Mahowald N. (2000) What caused the glacial/interglacial atmospheric pCO_2 cycles? *Rev. Geophys.* **38** (*2*), 159–189.

Bainbridge A. E., and GEOSECS Operations Group (1981) GEOSECS Hydrographic Data 1972–1973, National Science Foundation.

Barker S., and Elderfield H. (2002) Foraminiferal calcification response to glacial-interglacial changes in atmospheric pCO_2. *Science* **297,** 833–836.

Barnett M. O., Jardine P. M., Brooks S. C., and Selim H. M. (2000) Adsorption and transport of uranium(VI) in subsurface media. *Soil Sci. Soc. America J.* **64,** 908–917.

Barnola J. M., Raynaud D., Korotkevich V. S., and Lorius C. (1987) Vostok ice core provides 160,000 year record of atmospheric CO_2. *Nature* **329,** 408–413.

Berner W., Stauffer B., and Oeschger H. (1979) Past atmospheric composition and climate, gas parameters measured on ice cores. *Nature* **275,** 53–55.

Bijma J., Spero H. J., and Lea D. W. (1998) Oceanic carbonate chemistry and foraminiferal isotopes: New laboratory results. *Sixth International Conference on Paleoceanography,* 78.

Bijma J., Spero H. J., and Lea D. W. (1999) Reassessing foraminiferal stable isotope geochemistry: Impact of the oceanic carbonate system (experimental results). In *Uses of Proxies in Paleoceanography: Examples from the South Atlantic* (eds. G. Fischer and G. Wefer), pp. 489–512. Springer Verlag, Berlin-Heidelberg.

Bijma J., Hönisch B., and Zeebe R. (2002). Impact of the ocean carbonate chemistry on living foraminiferal shell weight: Comment on "Carbonate ion concentration in glacial-age deep waters of the Caribbean Sea" by W. S. Broecker and E. Clark. *Geochem. Geophys. Geosyst.* **3,** 1064, doi: 10.1029/20026C000388.

Billups K., and Spero H. J. (1995) Relationship between shell size, thickness, and stable isotopes in individual planktonic foraminifera from two equatorial Atlantic cores. *J. Foram. Res.* **25,** 24–37.

Boyle E. A. (1983) Manganese carbonate overgrowths on foraminifera tests. *Geochim. Cosmochim. Acta* **47,** 1815–1819.

Broecker W., and Clark E. (2001) An evaluation of Lohmann's foraminifera weight dissolution index. *Paleoceanography* **16,** 531–534.

Broecker W., and Clark E. (2002) Carbonate ion concentration in glacial-age deep waters of the Caribbean Sea. *Geochem. Geophys. Geosystems* **3,** 10.1029/2001GC000231.

Broecker W. S., and Clark E. (2003) Glacial-age deep sea carbonate ion concentrations. *Geochem. Geophys. Geosystems* **4,** 10.1029/2003GC000506.

Broecker W. S., and Peng T.-H. (1982) *Tracers in the Sea.* Lamont Doherty Geological Observatory.

Brook E. J., Harder S., Severinghaus J., and Bender M. (1999) Atmospheric methane and millenial scale climate change. In Mechanisms of Global Climate Change at Millenial Time Scales. By Peter U. Clark, R. S. Webb, and L. Lloyd Keigwin (eds). American Geophysical Union Monograph **112,** 165–176.

Chen C. T. (1984) Carbonate chemistry of the Weddell Sea. TR008, U. S. Department of Energy, Carbon Dioxide Research Division, Washington D. C. Data available online at http://cdiac.ornl.gov/ftp/ndp028/.

Chen J. H., Edwards R. L., and Wasserburg G. J. (1986) ^{238}U, ^{234}U, and ^{232}Th in seawater. *Earth Planet. Sci. Lett.* **80,** 241–251.

Chung G. S., and Swart P. K. (1990) The concentration of uranium in freshwater vadose and phreatic cements in a Holocene ooid cay—a method of identifying ancient water tables. *J. Sed. Pet.* **60,** 735–746.

Clark D. L., Hobart D. E., and Neu M. P. (1995) Actinide carbonate complexes and their importance in actinide environmental chemistry. *Chem. Rev.* **95** (*1*), 25–48.

Curry W. B., and Lohmann G. P. (1986) Late Quaternary carbonate sedimentation at the Sierra Leone Rise (eastern equatorial Atlantic Ocean). *Marine Geol.* **70,** 223–250.

Dekens P. S., Lea D. W., Pak D. K., and Spero H. J. (2002) Core top calibration of Mg/Ca in tropical foraminifera: Refining paleo-temperature estimation. *Geochem. Geophys. Geosyst.* **3,** 1022.

Delaney M. L., and Boyle E. A. (1983) Uranium and thorium isotopes in foraminiferal calcite. *Earth Planet. Sci. Lett.* **62,** 258–262.

Dickson A. G. (1990) Standard potential of the reaction: $AgCl_{2(s)} + 1/2H_{2(g)} = Ag_{(s)} + HCl_{(aq)}$, and the standard acidity constant of the ion HSO_4^- in synthetic seawater from 273.15 to 318.15 K. *J. Chem. Thermodyn.* **22,** 113–127.

Dickson A. G., and Millero F. J. (1987) A comparison of the equilibrium constants for the dissociation of carbonic acid in seawater media. *Deep-Sea Res.* **34,** 1733–1743.

Djogic R., Sipos L., and Branica M. (1986) Characterization of uranium(VI) in seawater. *Limnol. Oceanogr.* **31** (*5*), 1122–1131.

Gratz A. J., Hillner P. E., and Hansma P. K. (1993) Step dynamics and spiral growth on calcite. *Geochim. Cosmochim. Acta* **57,** 491–495.

Grenthe I. (1992). Chemical Thermodynamics of Uranium, edited by H. Wanner and I. Forest. Nuclear Energy Agency, Organization for Economic Cooperation and Development, Amsterdam, New York: North-Holland, New York, NY, 715 p.

Hamilton C. P. (1996). Gametogenic calcification in the planktonic foraminifera *Orbulina universa* and glacial to interglacial sea surface temperatures across the subtropical convergence in the southwest Pacific Ocean. M.S. thesis, University of California, Davis, 183 pp.

Hemming N. G., Reeder R. J., and Hart S. R. (1998) Growth-step selective incorporation of boron on the calcite surface. *Geochim. Cosmochim. Acta* **62,** 2915–2922.

Henderson G. M., and O'Nions R. K. (1995) (^{234}U/^{238}U) ratios in Quaternary planktonic foraminifera. *Geochim. Cosmochim. Acta* **59,** 4685–4694.

Hönisch B., Bijma J., Russell A. D., Spero H. J., Palmer M. R., Zeebe R. E., and Eisenhauer A. (2003) The influence of symbiont photosynthesis on the boron isotopic composition of foraminifera shells. *Marine Micropaleontology* **49,** 87–96.

Hsi C.-K. D., and Langmuir D. (1985) Adsorption of uranyl onto ferric oxyhydroxides: Application of the surface complexation site-binding model. *Geochim. Cosmochim. Acta* **49,** 1931–1941.

Indermühle A., Stocker T. F., Joos F., Fischer H., Smith J. H., Wahlen M., Deck B., Mastroianni D., Tschumi J., Blunier T., Meyer R., and Stauffer B. (1999) Holocene carbon-cycle dynamics based on CO_2 trapped in ice at Taylor Dome, Antarctica. *Nature* **398,** 121–126.

Katz A. (1973) The interaction of magnesium with calcite during crystal growth at 25-90°C and one atmosphere. *Geochim. Cosmochim. Acta* **37,** 1563–1586.

Kitano Y., and Oomori T. (1971) The coprecipitation of uranium with calcium carbonate. *Jr. Oceanog. Soc. Japan* **27,** 34–42.

Ku T. L. (1965) An evaluation of the $^{234}U/^{238}U$ method as a tool for dating pelagic sediments. *J. Geophys. Res.* **70,** 3457–3474.

Langmuir D. (1978) Uranium solution-mineral equilibria at low temperatures with applications to sedimentary ore deposits. *Geochim. Cosmochim. Acta* **42,** 547–569.

Lea D. W., and Martin P. A. (1996) A rapid mass spectrometric method for the simultaneous analysis of barium, cadmium, and strontium in foraminifera shells. *Geochim. Cosmochim. Acta* **60,** 3143–3149.

Lea D. W., Bijma J., Spero H. J., and Archer D. (1999) Implications of a carbonate ion effect on shell carbon and oxygen isotopes for glacial ocean conditions. In *Use of Proxies in Paleoceanography: Examples from the South Atlantic.* (ed. G. Fischer and G. Wefer). Springer Verlag, Berlin-Heidelberg. pp. 513–522.

Lea D. W., Mashiotta T. A., and Spero H. J. (1999b) Controls on magnesium and strontium uptake in planktonic foraminifera determined by live culturing. *Geochim. Cosmochim. Acta* **63,** 2369–2379.

Lewis E., and Wallace D. W. R. (1998) Program developed for CO_2 system calculations. Carbon Dioxide Information Analysis Center, Oak Ridge National Laboratory, U.S. Department of Energy.

Lohmann G. P. (1995) A model for variation in the chemistry of planktonic foraminifera due to secondary calcification and selective dissolution. *Paleoceanography* **10,** 445–457.

Lorens R. B. (1981) Sr, Cd, Mn, and Co distribution coefficients in calcite as a function of calcite precipitation rate. *Geochim. Cosmochim. Acta* **45,** 553–561.

Marchitto T. M., Lynch-Stieglitz J., Curry W. B., and Oppo D. W. (2001) Quantitative reconstruction of glacial/interglacial carbonate ion concentrations in the deep Pacific using Zn and Cd in benthic foraminifera. *EOS, Transactions, American Geophysical Union,* OS31E-03.

Marchitto T. M. J., Curry W. B., and Oppo D. W. (2000) Zinc concentrations in benthic foraminifera reflect seawater chemistry. *Paleoceanography* **15,** 299–306.

Martin P. A., Lea D. W., Mashiotta T. A., Papenfuss T., and Sarnthein M. Variation of foraminiferal Sr/Ca over Quaternary glacial-interglacial cycles: Evidence for changes in mean ocean Sr/Ca? *Geochem. Geophy. Geosys.* **1,** Paper Number 1999GC000006, 1999.

Mashiotta T. A., Lea D. W., and Spero H. J. (1999). Glacial-interglacial changes in subantarctic sea-surface temperature and $\delta^{18}O$-water using foraminiferal Mg. *Earth Planet. Sci. Lett.* **170,** 417–432.

Meece D. E. and Benninger L. K. (1993) The coprecipitation of Pu and other radionuclides with $CaCO_3$. *Geochim. Cosmochim. Acta* **57,** 1447–1458.

Mehrbach C., Culberson C. H., Hawley J. E., and Pytkowicz R. M. (1973) Measurement of the apparent dissociation constants of carbonic acid in seawater at atmospheric pressure. *Limnol. Oceanogr.* **18,** 897–907.

Millero F. J. and Sohn M. L. (1992) *Chemical Oceanography.* CRC Press.

Min G. R., Edwards R. L., Taylor F. W., Recy J., Gallup C. D., and Beck J. W. (1995) Annual cycles of U/Ca in coral skeletons and U/Ca thermometry. *Geochim. Cosmochim. Acta* **59,** 2025–2042.

Morse J. W. and Bender M. L. (1990) Partition coefficients in calcite: Examination of factors influencing the validity of experimental results and their application to natural systems. *Chem. Geol.* **82,** 265–277.

Mucci A. (1987) Influence of temperature on the composition of magnesian calcite overgrowths precipitated from seawater. *Geochim. Cosmochim. Acta* **51,** 1977–1984.

Mucci A. and Morse J. W. (1983) The incorporation of Mg^{2+} and Sr^{2+} into calcite overgrowths: Influences of growth rate and solution composition. *Geochim. Cosmochim. Acta* **47,** 217.

Mucci A., Morse J. W., and Kaminsky M. S. (1985) Auger spectroscopy analysis of magnesian calcite overgrowths precipitated from seawater and solutions of similar composition. *Am. J. Sci* **285,** 289–305.

Neftel A., Oeschger H., Swander J., Stauffer B., and Zumbrunn R. (1982) Ice core sample measurements give atmospheric CO_2 content during the past 40,000 years. *Nature* **295,** 220–223.

Paquette J. and Reeder R. J. (1995) Relationship between surface structure, growth mechanism, and trace element incorporation into calcite. *Geochim. Cosmochim. Acta* **59,** 735–749.

Petit J. R., Jouzel J., and Raynaud D. (1999) Climate and atmospheric history of the past 420,000 years from the Vostok ice core, Antarctica. *Nature* **399,** 429–436.

Reeder R. J. (1996) Interaction of divalent cobalt, zinc, cadmium, and barium with the calcite surface layer during crystal growth. *Geochim. Cosmochim. Acta* **60,** 1543–1552.

Reeder R. J., Nugent M., Lamble G. M., Tait C. D., and Morris D. E. (2000) Uranyl incorporation into calcite and aragonite: XAFS and luminescence studies. *Environ. Sci. Technol.* **34,** 638–644.

Reeder R. J., Nugent M., Tait C. D., Morris D. E., Heald S. M., Beck K. M., Hess W. P., and Lanzirotti A. (2001) Coprecipitation of uranium(VI) with calcite: XAFS, micro-XAS, and luminescence characterization. *Geochim. Cosmochim. Acta* **65** (*20*), 3491–3503.

Rink S., Kuhl M., Bijma J., and Spero H. J. (1998) Microsensor studies of photosynthesis and respiration in the symbiotic foraminifer *Orbulina universa*. *Marine Biology* **131,** 583–595.

Rosenthal Y., Field P., and Sherrell R. M. (1999) Precise determination of element/calcium ratios in calcareous samples using sector field inductively coupled mass spectrometry. *Analyt. Chem.* **71,** 3248–3253.

Rosenthal Y., Perron-Cashman C., Lear C, et al. (2004). Inter-laboratory comparison study of Mg/Ca and Sr/Ca measurements in planktonic foraminifera for paleoceanographic research. *Geochem. Geophys. Geosyst. 5,* Q0D09. doi: 10.1029/2003GCD00650.

Russell A. D., Emerson S., Mix A. C., and Peterson L. C. (1996) The use of foraminiferal U/Ca as an indicator of changes in seawater U content. *Paleoceanography* **11,** 649–663.

Russell A. D., Emerson S. R., Nelson B. K., Erez J., and Lea D. W. (1994) Uranium in foraminiferal calcite as a recorder of seawater uranium concentrations. *Geochim. Cosmochim. Acta* **58,** 671–681.

Sanyal A. and Bijma J. (1999) A comparative study of the northwest Africa and eastern equatorial Pacific upwelling zones as sources of CO_2 during glacial periods based on boron isotope paleo-pH estimation. *Paleoceanography* **14,** 753–759.

Shen G. T. and Dunbar R. B. (1995) Environmental controls on uranium in reef corals. *Geochim. Cosmochim. Acta* **59** (*10*), 2009–2024.

Sigman D. and Boyle E. A. (2000) Glacial/interglacial variations in atmospheric carbon dioxide. *Nature* **407,** 859–869.

Sigman D., McCorkle D. C., and Martin W. R. (1998) The calcite lysocline as a constraint on glacial/interglacial low-latitude production changes. *Global Biogeochem. Cycles* **12,** 409–427.

Spero H. J., Andreasen D. J., and Sorgeloos P. (1993) Carbon and nitrogen isotopic composition of different strains of *Artemia* sp. *Int. J. Salt Lake Res.* **2,** 133–139.

Spero H. J., Bijma J., Lea D. W., and Bemis B. E. (1997) Effect of seawater carbonate ion concentration on foraminiferal carbon and oxygen isotopes. *Nature* **390,** 497–500.

Spero H. J., Bijma J., Lea D. W., and Russell A. D. (1999) Deconvolving glacial ocean carbonate chemistry from the planktonic foraminifera carbon isotope record. In *Reconstructing Ocean History: A Window into the Future* (eds. F. Abrantes and A. Mix). Plenum.

Spero H. J. and Williams D. F. (1988) Extracting environmental information from planktonic foraminiferal $\delta^{13}C$ data. *Nature* **335,** 717–719.

Staudt W. J., Reeder R. J., and Schoonen M. A. A. (1994) Surface structural controls on compositional zoning of SO_4^{2-} and SeO_4^{2-} in synthetic calcite single crystals. *Geochim. Cosmochim. Acta* **58,** 2087–2098.

Stoll H. M., Schrag D. P., and Clemens S. C. (1999) Are seawater Sr/Ca variations preserved in Quaternary foraminifera? *Geochim. Cosmochim. Acta* **63,** 3535–3547.

Stoll H. M., Klaas C. M., Probert I., Encinar J. R., and Alonso J. I. G. (2002) Calcification rate and temperature effects on Sr partitioning in coccoliths of multiple species of coccolithophorids in culture. *Global Planet. Change* **34,** 153–171.

Swart P. K. and Hubbard J. A. E. B. (1982) Uranium in scleractinian coral skeletons. *Coral Reefs* **1,** 13–19.

Tamon H., Mori H., Ohyama S., and Okazaki M. (1990) Correlation of adsorption equilibrium of uranium by taking into account its chemical species in seawater. *J. Chem. Eng. Japan* **23,** 433–438.

Zeebe R. E. (2001). Seawater pH and isotopic paleotemperatures of Cretaceous oceans. *Palaeogeogr. Palaeoclimatol. Palaeoecol.* **170,** 49–57.

Table A1. Sample Me/Ca ratios, experimental conditions, and mean (±1 standard error) length, weight, and wall thickness of cultured *O. universa*.[a]

Sample name	T (°C)	$[CO_3^{2-}]$ μmol kg^{-1}	Dissolved calcite weight (μg)	Mean length (μm)	Mean weight (μg)	Wall thickness (μm)	*n*	Mg/Ca (mmol mol^{-1})	Sr/Ca (mmol mol^{-1})	U/Ca (nmol mol^{-1})
AR1-A	22	213	19	493 ± 11	18 ± 1	10	5	5.82	1.27	*17.2*
AR1-B	22	213	61	493 ± 17	23 ± 1	13	5	6.12	1.25	7.0
AR1-C	22	213	58	522 ± 16	27 ± 1	14	6	8.23	1.31	14.6
AR1-D	22	213	117	564 ± 14	34 ± 1	15	9	7.93	1.27	9.1
AR1-E	22	213	58	640 ± 42	38 ± 1	13	4	6.98	1.23	9.9
AR1-3	22	213	61	600 ± 13	53 ± 5	20	2	6.54	1.31	11.4
AR1-5	22	213	62	667 ± 90	73 ± 15	23	2+	7.03	1.25	9.6
AR3-A	22	301	14	427 ± 8	15 ± 2	11	3	5.26	1.29	*11.8*
AR3-B	22	301	32	467 ± 26	25 ± 1	16	2	5.34	1.30	8.3
AR3-C	22	301	30	520 ± 16	29 ± 1	15	3	5.66	1.31	9.2
AR3-D	22	301	124	568 ± 18	33 ± 1	14	8	7.27	1.31	7.9
AR3-E	22	301	180	575 ± 8	38 ± 1	16	10	6.84	1.33	6.3
AR3-F	22	301	231	573 ± 12	43 ± 1	18	6	5.95	1.31	6.3
AR3-H	22	301	88	653 ± 40	59 ± 1	19	2	8.08	1.33	10.9
AR3-I	22	301	71	634 ± 47	69 ± 1	24	2	7.67	1.33	9.2
AR4-A	22	399	65	437 ± 26	22 ± 2	16	5	5.64	1.34	7.2
AR4-B	22	399	136	477 ± 4	28 ± 1	17	11	6.65	1.38	5.9
AR4-C	22	399	65	537 ± 12	32 ± 1	15	4	6.20	1.36	5.9
AR4-D	22	399	34	540 ± 7	37 ± 1	18	2	6.93	1.38	9.0
AR4-E	22	399	96	520 ± 12	44 ± 2	23	4	6.34	1.39	5.4
AR4-F	22	399	53	609 ± 32	61 ± 2	23	3	6.74	1.35	6.9
AR5-A	22	480	48	467 ± 15	25 ± 2	16	4	4.96	1.41	*17.3*
AR5-B	22	480	21	506 ± 1	36 ± 1	20	3	5.46	1.39	6.2
AR5-C	22	480	91	525 ± 12	47 ± 1	24	3	7.49	1.40	3.9
AR5-D	22	480	143	567 ± 14	55 ± 2	24	4	7.65	1.43	5.2
AR5-E	22	480	80	587 ± 16	64 ± 2	26	3	6.15	1.39	5.0
AR5-F	22	480	79	627	94	35	1	5.38	*1.28*	6.5
BH1b	22	182		461 ± 21	20 ± 3	10	1	5.23	1.22	4.1
BH1c	22	182	39				3	9.75	1.36	6.2
BH1d	22	182	28				2	5.50	1.22	5.3
BH1e	22	182	18				2	8.07	1.26	*3.5*
BH3b	22	76	34	481 ± 27	24 ± 3	12	3	10.5	1.25	20.6
BH3c	22	76	27				2	10.1	1.28	14.2
BH3d	22	76	*6*				*1*	*7.63*	*1.19*	*10.8*
BH6a	22	111	48	491 ± 19	29 ± 7	14	1	9.69	1.29	10.6
BH6b	22	111	28				2	4.96	1.18	9.6
BH6c	22	111	38				2	9.10	1.24	12.6
BH2b	22	196	32	536 ± 22	35 ± 4	14	1	*11.6*	1.32	8.5
BH2c	22	196	38				2	6.38	1.26	10.2
BH2d	22	196	39				2	6.32	1.25	6.6
BH2e	22	196	31				1	*10.186*	*1.363*	6.5
BH5a	22	311	86	559 ± 32	48 ± 12	19	1	*14.4*	*1.45*	5.8
BH5b	22	311	41				1	8.03	1.29	6.9
BH5c	22	311	29				1	5.75	1.29	4.5
BH5d	22	311	30				1	7.61	1.37	4.5
BH4b	22	468	55	536 ± 17	44 ± 5	19	1	6.33	1.36	5.0
BH4c	22	468	53				2	6.35	1.40	3.9
BH4d	22	468	29				3	8.21	1.41	5.1
BH4e	22	468	50				1	6.94	1.42	2.9
AR6-T1	15	170	15	418 ± 29	13 ± 3	7 ± 3	3	3.35	1.23	*17.3*
AR6-T2	15	170	22	369 ± 23	15 ± 2	11 ± 1	3	3.86	1.24	10.1
AR6-T3	15	170	33	391 ± 32	18 ± 3	12 ± 1	3	3.49	1.24	8.9
AR6-T4	15	170	31	467 ± 67	32 ± 9	18 ± 1	2	3.44	1.24	8.9
AR27-T16	18	166	20	527 ± 34	28 ± 3	11 ± 0	2	5.19	1.25	*15.7*
AR27-T18	18	166	30	447 ± 47	23 ± 4	13 ± 0	2	4.20	1.25	8.7
AR27-T19	18	166	34	453 ± 0	24 ± 1	13 ± 0	2	4.92	1.29	8.6
AR27-T20	18	166	22	481 ± 47	28 ± 4	14 ± 1	2	4.80	1.27	6.9
AR27-T21	18	166	21	467 ± 33	30 ± 4	16 ± 0	2	6.61	1.34	9.6
AR27-T22	18	166	44	517 ± 17	46 ± 4	17 ± 0	2	3.94	1.25	7.7
AR27-T23	18	166	42	477 ± 44	35 ± 5	19 ± 1	2	5.49	1.28	7.7
AR12-T6	25	216	6	447 ± 87	16 ± 5	7 ± 0	2	7.65	1.26	*20.7*
AR12-T7	25	216	33	547 ± 0	27 ± 1	10 ± 0	2	8.31	1.28	13.5
AR10-12-T8	25	216	9	534 ± 54	28 ± 3	12 ± 1	2	10.7	1.33	*13.4*
AR10-T9	25	216	24	567 ± 20	35 ± 1	13 ± 0	2	9.33	1.33	8.6

Table A1. (Continued)

Sample name	T (°C)	[CO_3^{2-}] μmol kg^{-1}	Dissolved calcite weight (μg)	Mean length (μm)	Mean weight (μg)	Wall thickness (μm)	*n*	Mg/Ca (mmol mol^{-1})	Sr/Ca (mmol mol^{-1})	U/Ca (nmol mol^{-1})
AR12-T10	25	216	58	534 ± 14	33 ± 1	14 ± 0	2	11.4	1.35	12.4
AR12-T11	25	216	61	494 ± 14	29 ± 1	14 ± 0	2	8.82	1.30	8.5
AR10-12-T12	25	216	17	500 ± 7	30 ± 1	14 ± 0	2	10.6	1.29	*17.4*
AR12-T13	25	216	24	554 ± 7	37 ± 1	15 ± 0	2	8.60	1.31	9.2
AR12-T14	25	216	63	514 ± 34	33 ± 4	15 ± 0	2	10.7	1.29	6.3
AR12-T15	25	216	25	540 ± 20	36 ± 2	15 ± 0	2	9.94	1.32	7.3

[a] Values in italics were not included in means. *n* refers to number of foraminifera in the sample.